Supplemental Material

The PMI Predictor – a Web App Enabling Green-by-Design Chemical Synthesis

Alina Borovika[1*], Jacob Albrecht[1], Jun Li[1], Andrew S. Wells[2], Christiana Briddell[3], Barry R. Dillon[4], Louis J. Diorazio[5], James R. Gage[6], Fabrice Gallou[7], Stefan G. Koenig[8], Michael E. Kopach[9], David K. Leahy[10], Isamir Martinez[3], Martin Olbrich[11], Jared L. Piper[12], Frank Roschangar[13], Edward S. Sherer[14], Martin D. Eastgate[1].

Table of Contents

App Description

The Shiny[1] application was developed to estimate PMI for any synthetic process and is comprised of three main segments – **Process Definition**, **Step PMI Information**, and **Results**. Descriptions of each segment, presented on the app as separate tabs, are outlined below.

Process Definition

Process Definition (Figure S2, [1]) is based on defining the synthetic route to the final product (API). To facilitate visualization and calculation of cumulative PMI, the synthetic sequence is treated as a graph of nodes representing the chemical intermediates connected by arrows representing the direction of the synthetic steps. For highly convergent syntheses, the graph will be a tree where each starting material leaf feeds into a single product at the root of the synthesis tree. This is facilitated by assigning each intermediate a unique label, with arbitrary letters currently used as labels in the app.

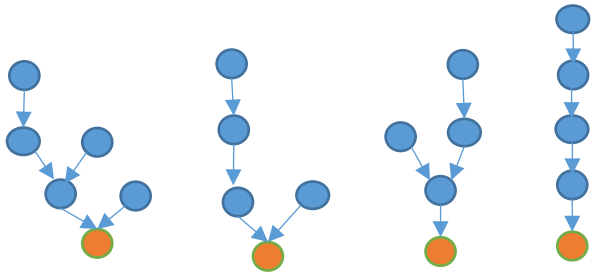

Figure S1. Demonstration of different topological synthetic pathways.

Next, the input for each chemical transformation is listed with its corresponding output, equivalent to describing the beginning and end of each arrow in the graph. For each transformation, a range of stoichiometry values may be entered to indicate a range of the possible molar ratios of each input to the step output. Ultimately, it is the user's choice to define what is considered to be a "starting material", however, the ACS GCIPR recommends to show synthesis of all components that are more expensive than $100/mol or that are not commercially available.

Given the list of inputs and outputs, the number and sequence of reaction steps is inferred and the synthetic route can be generated as a graph. Because the app was developed to support synthetic route planning for a single pharmaceutical drug substance, the synthesis tree must be convergent or linear, with a single product. Divergent routes (with two or more final products), or circular route definitions are not supported

in the app. Once the list of the intermediates and their stoichiometry is defined, the next tab generates the synthesis tree and allows for entry of the step information.

Step PMI Information

The next step in defining the proposed process is to specify molecular weights for each of the starting materials, intermediates, and final product (Figure S2, [2]). From the graph, each of the synthesized intermediate products are assumed to be produced in a single step, with a range of possible step PMI and molar yields. Custom ranges for PMI and yield may be used for existing routes, or preset ranges based on the published performance of chemistry classes are available to evaluate hypothetical routes. With this information, a system of equations to describe the masses of intermediates required at each step is defined. This system of equations is solved within each Monte Carlo iteration to estimate the cumulative PMI for the route on the final tab of the app.

App Results

In the final step of the app, a Monte Carlo simulation is used to incorporate the historical ranges of chemistry yield and PMI to calculate a distribution of cumulative PMI for the route. The min and max ranges are interpreted as intervals of a bivariate normal distribution of step PMI and step yield (99% as the default), a random sample is pulled from this distribution for each Monte Carlo iteration. Empirically, we have observed a negative correlation between step yield and step PMI, a correlation of -0.53 is used by default for the bivariate normal sampling. With values for each step in the synthetic sequence, each Monte Carlo iteration will have a calculated value of the cumulative PMI. The simulation results are plotted as histograms to show the distribution of predicted cumulative PMI with summary statistics (median and 95% interval) to provide process development teams with a range of process performance ((Figure S2, [3], [4]). The range of cumulative PMIs calculated provides realistic estimates for worst-case and best-case greenness and can be used to rank different proposed routes as well as to benchmark selected routes during development.

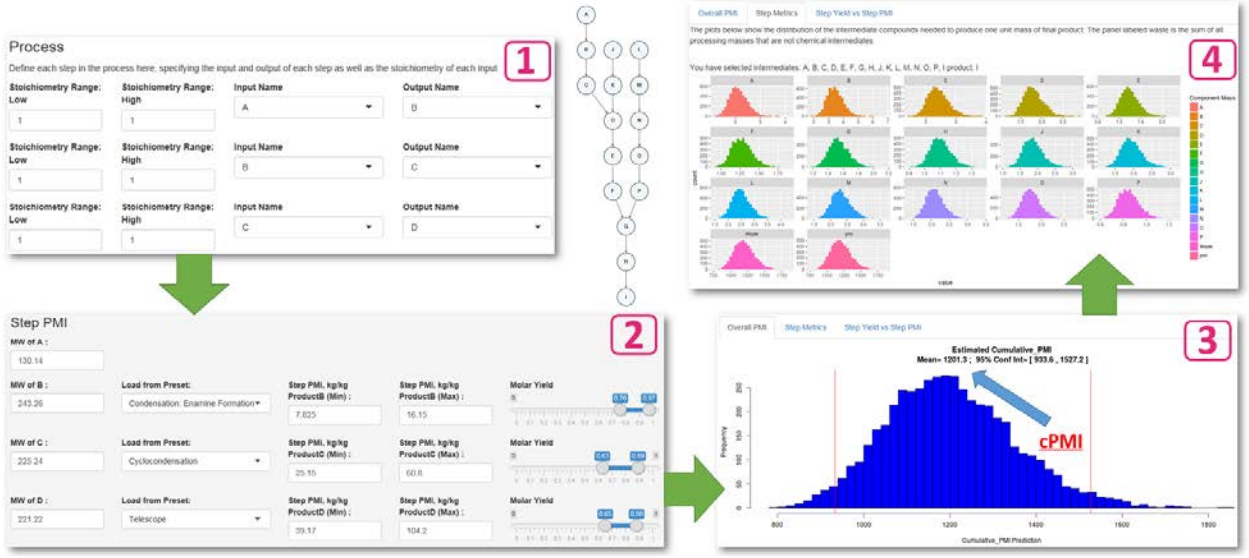

Figure S2. Screenshots of the web app. [1] Define the synthesis tree and stoichiometry. [2] Define reaction PMI and yield ranges based on reaction subtypes. [3] Obtain predicted cPMI histogram. [4] Obtain step metrics for all steps.

Scenario I example. Using BMS Brivanib example (Entry I in Discussion Table 1.) below we illustrate the application of the app to obtain the cPMI, and compare to the traditional cPMI calculator. Here the synthetic sequence to intermediate D was used. The corresponding step PMI and yield for each of the step shown in the following table:

Rxn	Step PMI	Yield
A→B	22	73.4%
B→C	47.7	67.5%
J→K	76	83.3%
C+K→D	97.8	81.5%

Set up the tool as follows:

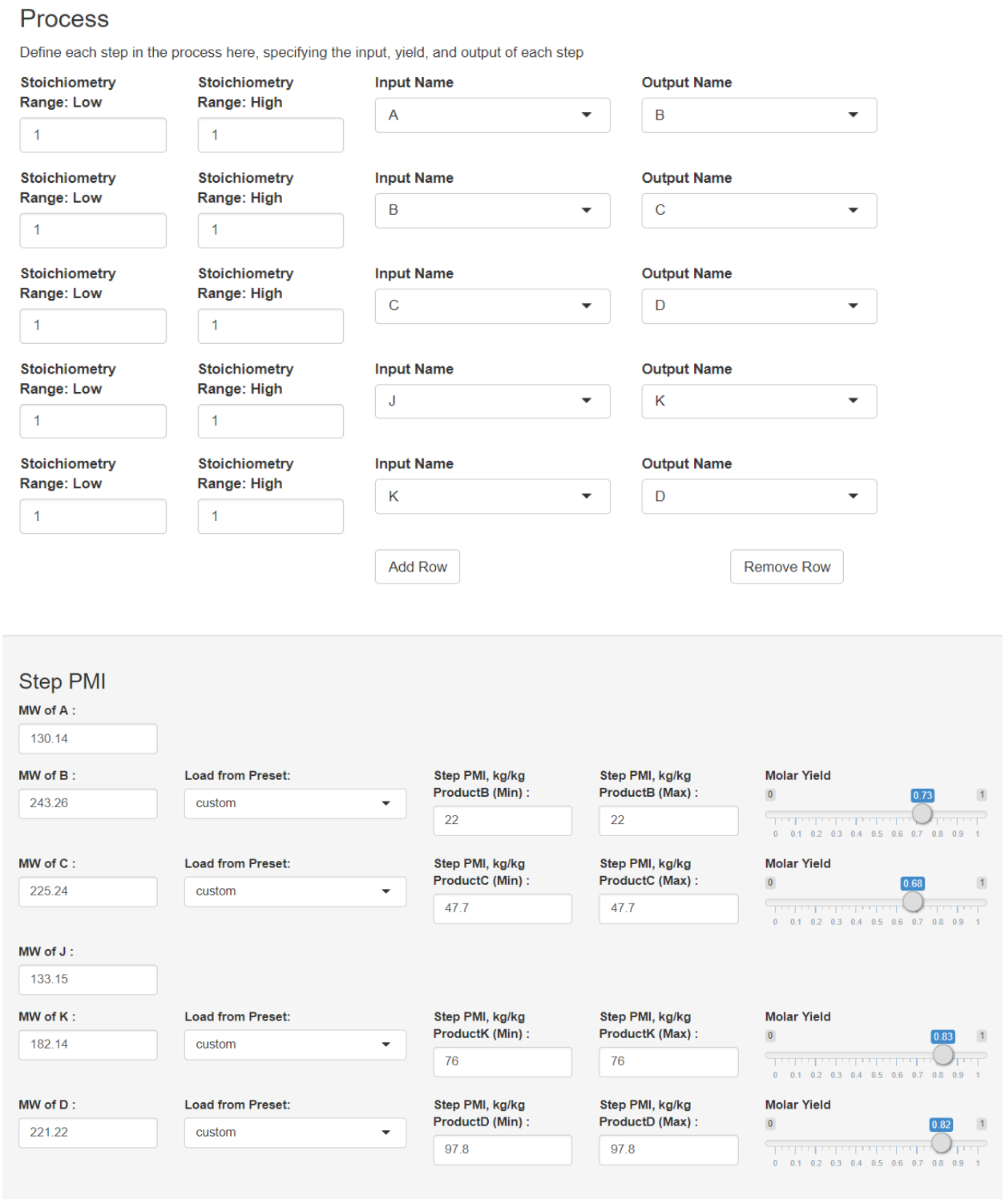

The overall cPMI for this sequence from the traditional calculator was 274 and this tool gave 273.

Scenario II example. The PMI Prediction Calculator app allows the user to incorporate parts of the synthetic sequence with limited or no detailed process info, to holistically assess the sustainability of the entire synthetic network, starting from raw materials with the threshold cost of $100 per mole defined. In this example we estimate cPMI for the Brettphos ligand synthesis based on the literature.[2] The synthesis included the telescoped process from 1,4-dimethoxy-2-fluorobenzene (**B**) and 2,4,6-triisopropylbromobenzene (**E**), followed by reacting with chlorodicyclohexylphosphine (**G**). The two step processes showed 63% yield with step PMI 158 and last step 80% yield and step PMI 92, respectively. Since the reported starting materials are priced above $100/mol, we introduced additional four steps (Scheme S1, highlighted in blue) in the synthesis to satisfy the selection criteria set by Roschangar *et. al*[3]. Thus, 1,4-dimethoxy-2-fluorobenzene **(B)** was prepared by oxidation, followed by methylation using ortho-fluorophenol **(A)**.[4] The yield for the telescoped process was reported around 45%. Based on this information, along with literature available synthesis of **G**, we used our PMI Prediction Calculator app to estimate the cPMI for this Brettphos ligand.

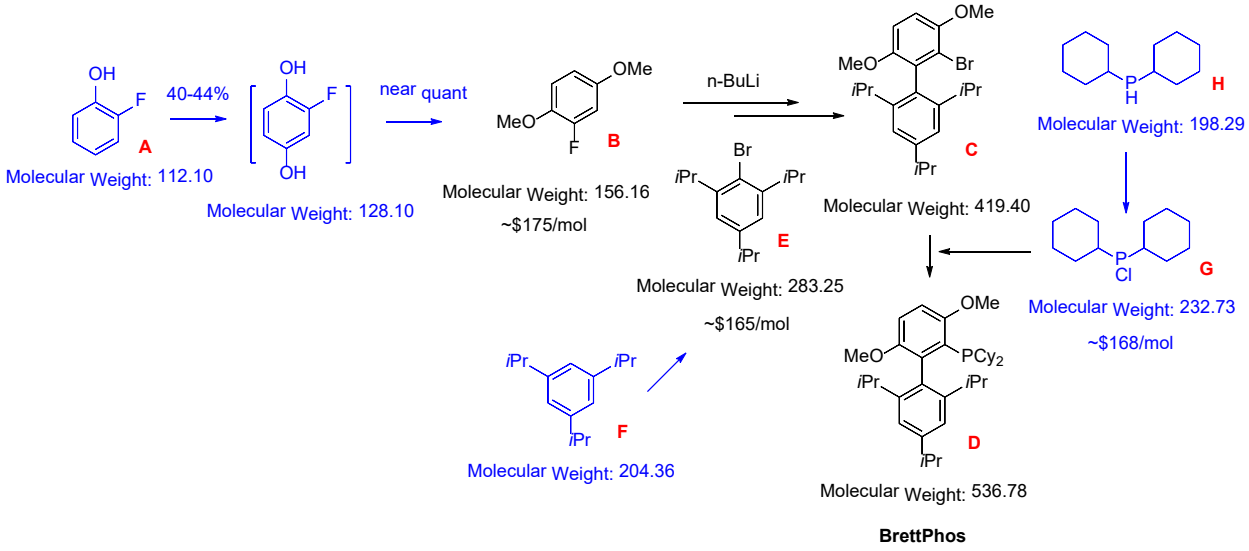

Scheme S1. Synthesis of Brettphos

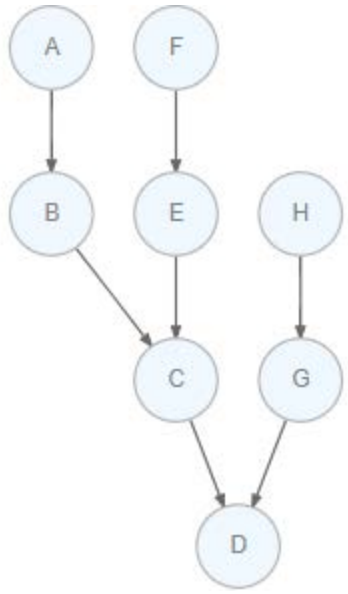

PMI Calculator | 1. Define Process | 2. PMI Values | 3. Results

Process

Define each step in the process here, specifying the input, yield, and output of each step

Stoichiometry Range: Low	Stoichiometry Range: High	Input Name	Output Name
1	1	A	B
1	1	B	C
1	1	C	D
1	1	F	E
2	2	E	C
1	1	H	G
1.09	1.09	G	D

Add Row | Remove Row

Following the steps outlined above (Figure S2), we defined reaction topology along with stoichiometry. In the available procedure two equivalent of 2,4,6-triisopropylbromobenzene (**E**) is used. We then defined reaction PMI and yield ranges based on reaction subtypes. In cases where some step PMI and yield info is available, actual values can be selected. Thus, for the first step, we selected observed 40~45% yield range based on the literature precedents, but used the generic step PMI range from the telescope type due to the absence of PMI info for these reactions. For the next telescoped step to make **C**, we chose the existing process info (step PMI 158; yield 63%).

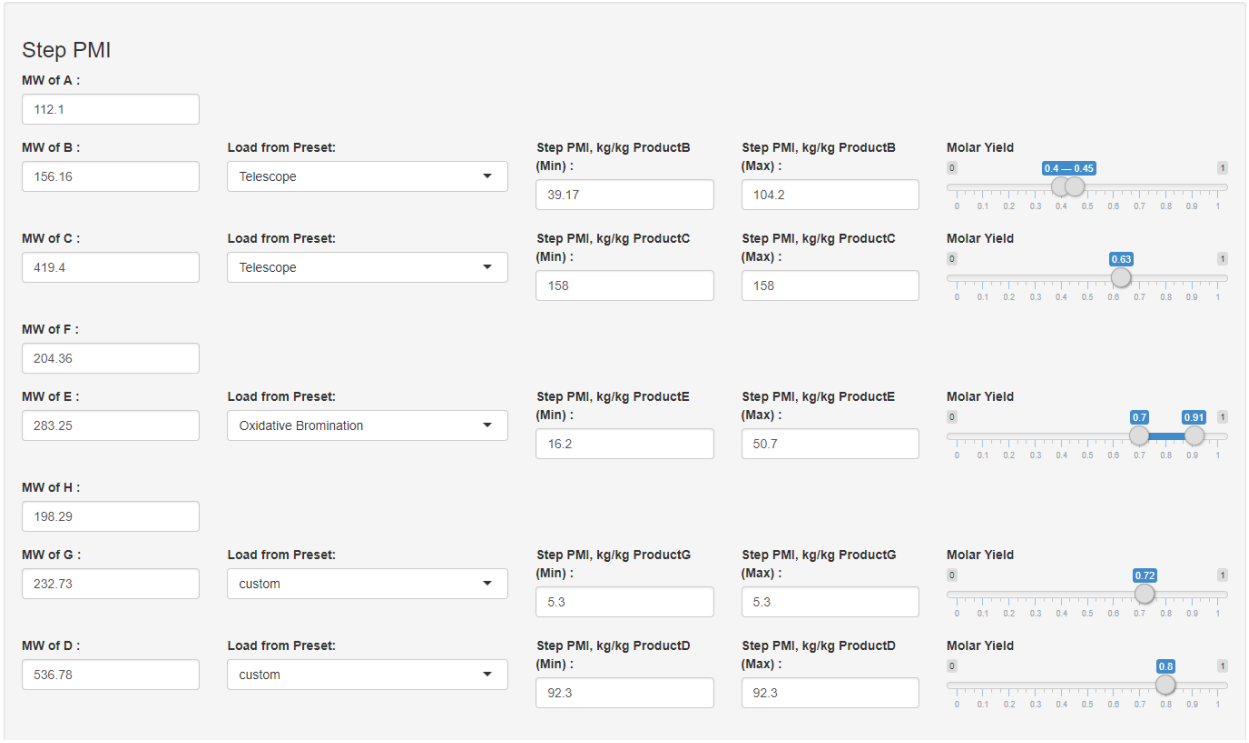

The calculated cPMI is 357 and 95% CI [326,388], which is 45% larger than the originally reported 2-step synthesis (cPMI 247), and we believe is a more accurate estimation of the actual synthetic efficiency for this ligand.

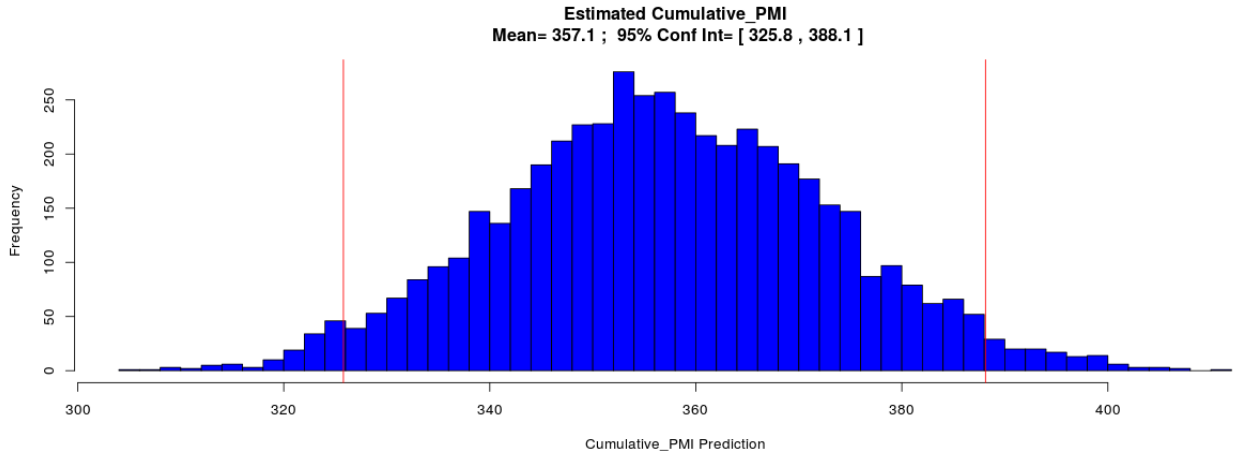

Scenario III Example. While other Excel-based step PMI and cPMI calculators have previously been developed, our web application based on the dynamic reacting program Shiny app[5] can be used to easily establish reaction networks with any intricate topological structures reflecting different convergent synthesis plans. It also allows the use of the well-established scale-up PMI and yield stats info from each reaction subtypes collected from this ACS GCI-led industrial collaborative efforts to quickly construct the network to probe the synthetic efficiency. As one can see from the previous example, this app allows to use either range or single numbers as inputs. Based on the chemists' experiences or knowledge, more adequate ranges can be chosen to override existing ranges. The flexibility of the app allows synthetic chemists to plug and play with the reaction types and their parameters to help envision the synthetic efficiency by assessing mass-based environmental impact and throughput of proposed synthetic routes.

Data Mining

The data was collected by individual companies through manual extraction and filtration of the raw data from industrial operational reports from their own processes. This extensive data set contains valuable information about general trends in chemical manufacturing in pharmaceutical industry and point to areas of improvement for the PMI Prediction Calculator. Overall we observed somewhat uneven distribution of data entries based on reaction categories (Figure S3). Nearly ¼ of reactions falls under category "other" of which 57% of the entries fall under "telescope" sub-category (a telescope is a sequence of chemical reactions performed without isolation of intermediates). The rest of the "other" includes 18% recrystallization, 8% salt formation, 4% classical resolution, 3% salt break, 2% chromatograph, 2% form conversion and etc. On the other hand, a few reaction categories ended up being underpopulated, such as

"C-M bond forming", "Hydration/Dehydration", and "Rearrangement", presumably pointing to either low popularity of these reactions in pharmaceutical manufacturing, or being part of telescoped processes. It is our goal to continuously keep improving the prediction calculator and perform additional data collection draws to populate the underrepresented reaction categories.

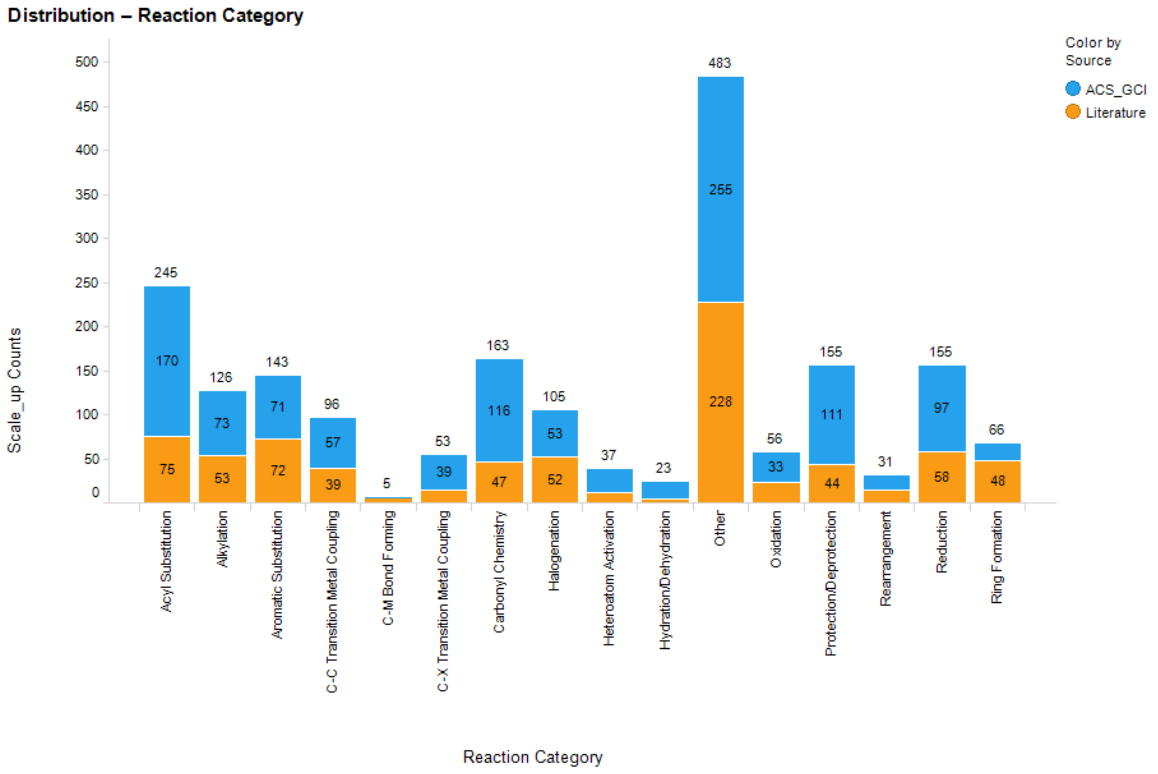

Figure S3. Distribution of number of scale-up reactions across sixteen major reaction categories.

Pharmaceutical synthesis is significantly more wasteful mainly due to the compounded effects of stringent regulatory compliance, increasing complexity of the active pharmaceutical ingredient (API) molecules, and speed-to-patient pressure under highly competitive health care market. Thus, median step PMI across this cross-company data set is 38, which translates to thirty eight kilograms of input materials combined for producing one kilogram of product in a single chemical processing step – an expected value based on historical approximation (Figure S4). Interestingly, when we subset the data by project development phases, we observe that typical step PMI for preclinical stage projects is ~27, while it nearly doubles to median ~51 in the ensuing phase I clinical stage projects. Low preclinical PMI can be rationalized through the understanding that preclinical deliveries do not require stringent quality control. It is generally known that additional purification procedures can dramatically increase PMI. Since Phase-I campaign is typically scheduled shortly after preclinical delivery, and results in fit-for-purpose strategies applied to the existing synthesis to ensure impurity control, which inevitably increases waste volume and PMI. Effect of additional

quality controls can also be observed in API step that includes protocols for controlling material purity, morphology, and particle size. Such additional manipulations result in increase in waste – median API step PMI is 50, which is 35% higher than non-API steps (37). Median step PMIs in Phase II up to commercial stage are similar (32-34), with significant improvement potentially resulted from either route innovation or process optimization to deliver more efficient and sustainable processes.

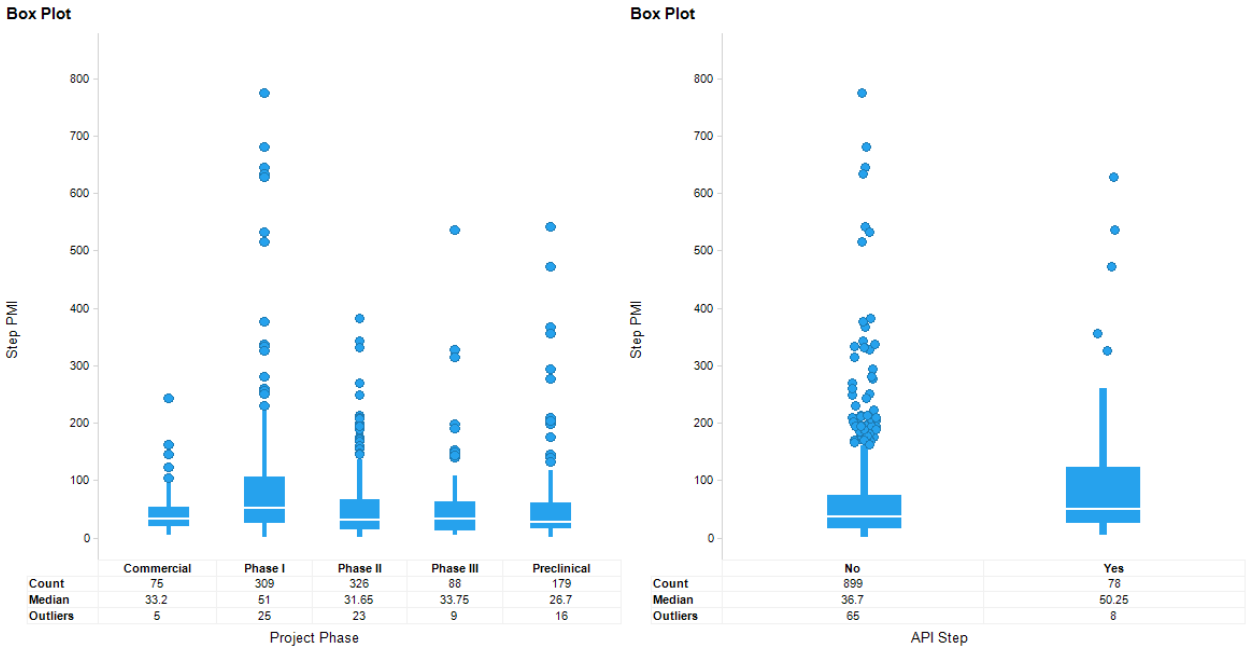

Figure S4. Step PMI distribution and statistics for different development phases and whether it is API step (outliers are partially displayed)

Analysis of the data acquired through literature search provided us with additional insights on breakdown of the chemical step processes. We attributed 65% of median step PMI to reaction workup - product purification and isolation. Further data analysis on step PMI subset by reaction subcategories based on number of counts in the dataset showed that *telescoped reaction, amidation, and deprotection* are the top three most populated subcategories. Figure S5 shows top 10 most popular reaction subtypes ranked by median PMI. Excluding telescoped reaction, top 6 reaction subtypes ranked in the following descending order by median PMI (transition metal-catalyzed C-N coupling > nitro reduction > heterocycle formation (cyclocondensation) > deprotection > amidation > Suzuki coupling). This list of top reaction subtypes is very much in line with the recent analysis of chemical reactions used by the medicinal chemistry based on the occurrences in the publication and US patents.[6] Transition metal catalyzed coupling reactions such as

C-N and Suzuki couplings have been used prominently in large scale pharmaceutical manufacturing.[7] It is interesting to see C-N coupling has the larger median PMI at 61 than Suzuki coupling at 37. Presumably, metal removal from nitrogen-rich heterocycles formed from C-N coupling tends to be more volume inefficient due to either poor solubility or strong metal chelation to the substrate compared to Suzuki product. Surprisingly, the nitro reduction gave median PMI at 50, without detailed info from the dataset we suspect that more cases involving reduction with stoichiometric amount of reductants rather than catalytic hydrogenation might influence the data. Overall high PMIs are typically observed for reactions that are either concentration dependent (i.e., Ring closing metathesis, RCM[8]), producing significant amount of side products (e.g. Mitsunobu), or impurities that are difficult to remove (Pd-catalyzed cross-coupling reactions). In Figure S4, we show top 10 largest PMI reaction subtypes by median regardless of the counts in the dataset. Here it is confirmed that ring closing metathesis (RCM) gave the largest median PMI at 598, followed by hydration/dehydration at 132, Sandmeyer reaction at 121, Mitsunobu 113, and direct arylation 88 in the top 5 group. More scale-up data are needed especially in under-represented reaction subtypes to improve our understanding of the PMI trends by reaction and workup.

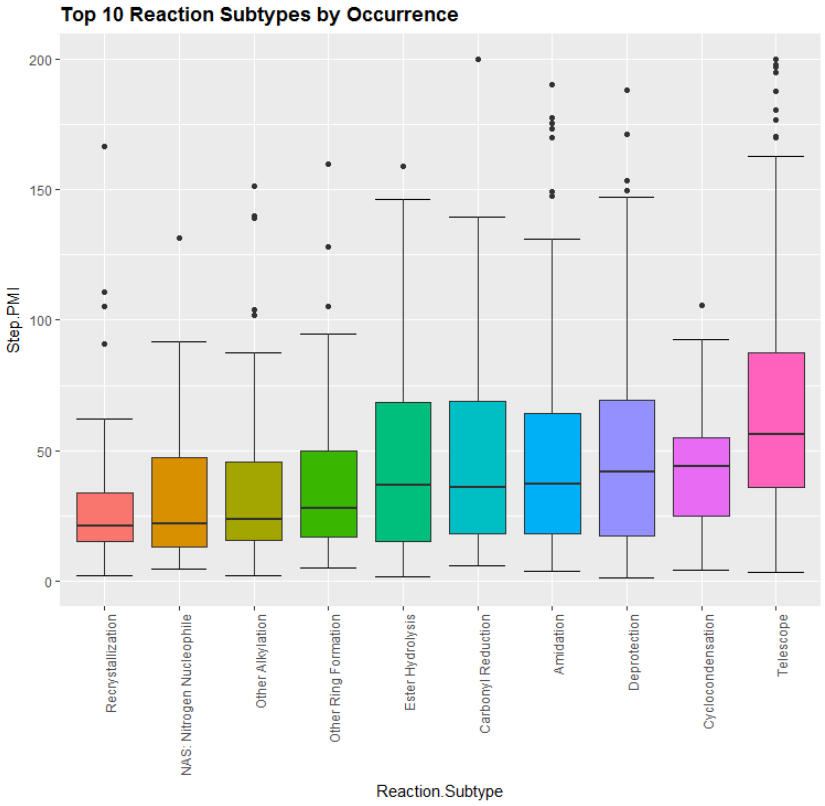

Reaction.Subtype	Counts	Median.PMI
Recrystallization	*85*	*21*
NAS: Nitrogen Nucleophile	*45*	*23*
Other Alkylation	*61*	*25*
Other Ring Formation	*49*	*28*
Ester Hydrolysis	*42*	*36*
Carbonyl Reduction	*39*	*37*
Amidation	*120*	*39*
Deprotection	*90*	*42*
Cyclocondensation	*42*	*46*
Telescope	*272*	*59*

Figure S5. Step PMI distribution subset by top 10 major reaction subtypes based on occurrences in the collected dataset.

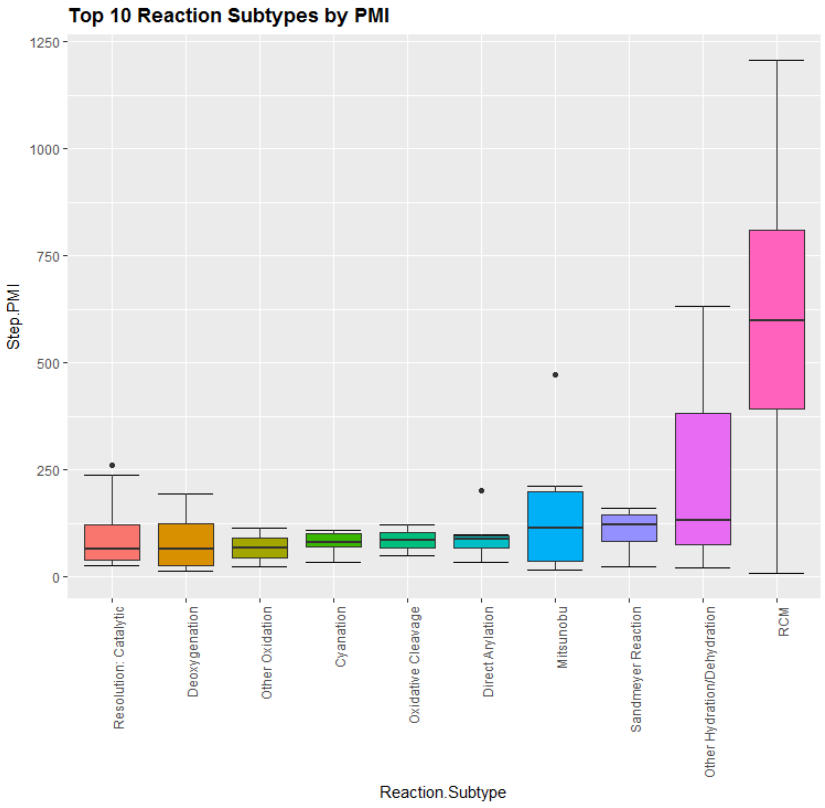

Reaction.Subtype	Counts	Median.PMI
Resolution: Catalytic	*8*	*65*
Deoxygenation	*4*	*66*
Other Oxidation	*2*	*68*
Cyanation	*9*	*81*
Oxidative Cleavage	*2*	*86*
Direct Arylation	*7*	*88*
Mitsunobu	*7*	*113*
Sandmeyer Reaction	*4*	*121*
Other Hydration/Dehydration	*3*	*132*
RCM	*4*	*598*

Figure S6. Step PMI distribution subset ranked by median PMI from all reaction subtypes in the collected dataset.

Besides the learnings from the generic characteristics of the step PMI and attributed workup under different reaction categories and subtypes, the analysis also quantified the benefits of telescoped processing (Figure S7). For telescoped processes, well-designed large-scale sequential chemical transformations without isolating the intermediates were shown to significantly reduce waste in pharmaceutical manufacturing. The median step PMI for telescoped 2-transformation process is around 27 and 4-transformation process is around 22, which are 24% and 42% reduction, respectively, comparing to single-transformation processes on per transformation basis. This again confirms our previous statement that additional purification steps can significantly increase PMI – the fewer intermediates are isolated, the lower the PMI. It is culminated in the recent literature[9] where seven-step telescoped scale-up process without isolating any intermediates has been demonstrated in one of the HCV drugs' synthesis.

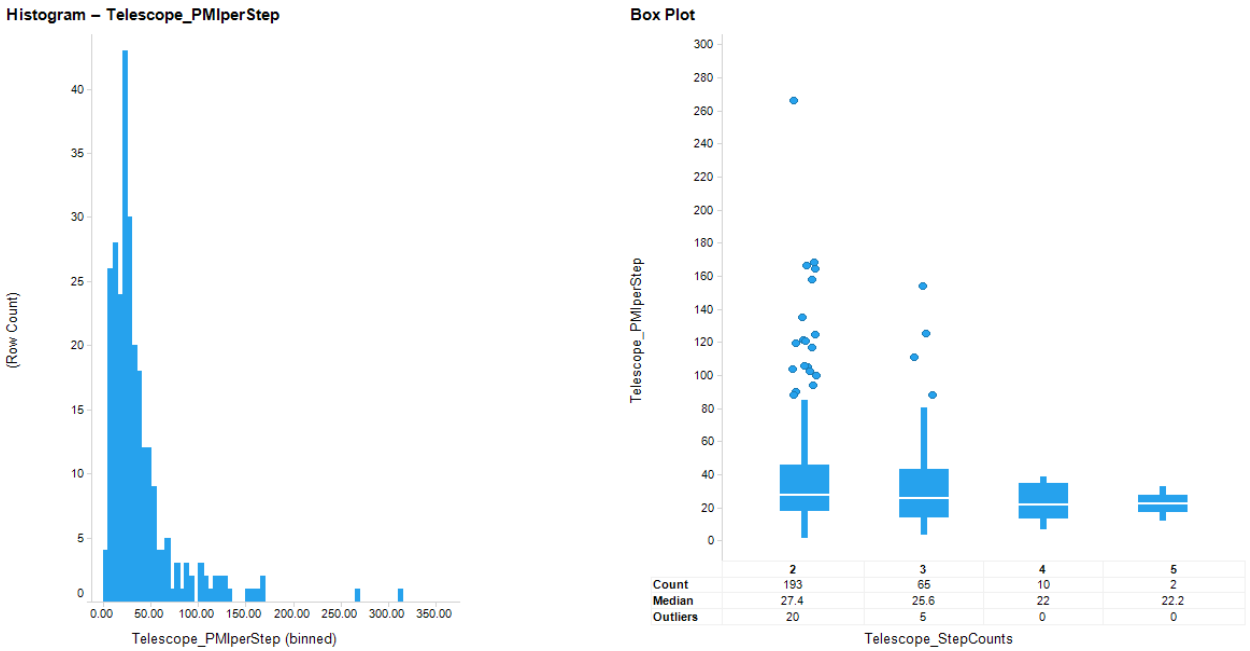

Figure S7. PMI per transformation distribution in telescoped processes

In collaboration with the GCIPR, this tool was further expanded with the goal of improving the predictive capabilities of the model, enable better decision making in route design, and to increase access and usage of the tool through development of a web-based tool.

Permutation Test Statistical Info

Due to the small sample sizes of the projects from early and mid_late development stages used in the group comparison, we chose the non-parametric permutation test to allow us to reject or not reject the null hypothesis of no difference between the model errors from two development stages. The R code used for the analysis is shown below:

```
#Model errors from two development stages
y1<-c(0.027624,-0.14747,-0.08868,-0.36287,-0.36021,-0.53644,-0.43178) #Group A
y2<-c(-0.1922,-0.03659,0.212121,-0.62722,0.359712,0.431315,0.910053,1.107784) #Group B
#Permuation test on the median differences between two groups
set.seed(222)
a<-y1
b<-y2
combined <- c(a,b)
# Observed difference
diff.observed <- median(b) - median(a)
number_of_permutations <-10000
diff.random <- NULL
for (i in 1 : number_of_permutations) {
  # Sample from the combined dataset without replacement
```

```
  shuffled <- sample (combined, length(combined))
  a.random <- shuffled[1 : length(a)]
  b.random <- shuffled[(length(a) + 1) : length(combined)]
  diff.random[i] <- median(b.random) - median(a.random)
}
# P-value is the fraction of how many times the permuted difference is equal or more extreme than the
observed difference
pvalue <- sum(abs(diff.random) >= abs(diff.observed)) / number_of_permutations
print (pvalue)
```

This provides the p-value of 0.0125.

As a comparison, we can also use Welch test assuming normality and unequal variance between these two groups and evaluate the difference between the mean of the model errors from the two groups. The Welch Two sample t-test showed p-value of 0.03292 [t.test(y1,y2, var.equal=FALSE)], supporting the alternative hypothesis of true difference in means is not equal to 0.

Selected Examples for App Performance Evaluation

Entry 1[10]

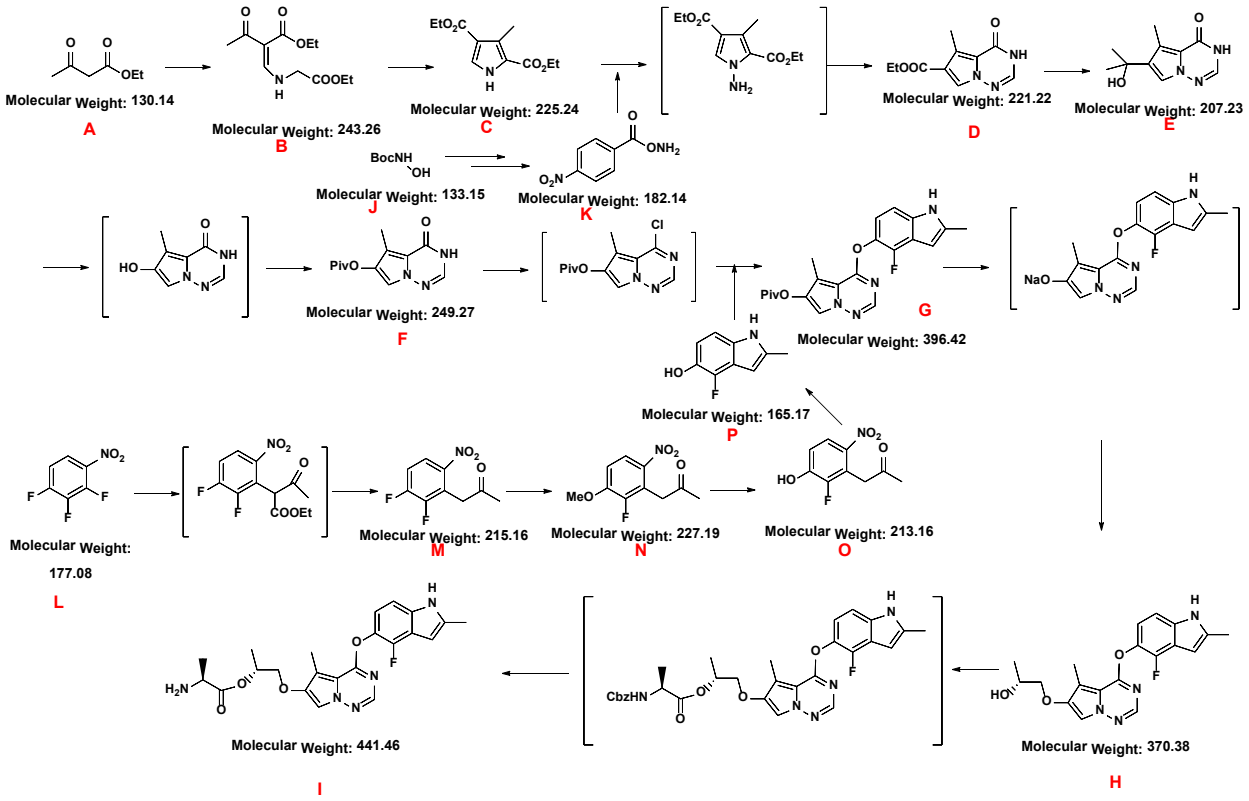

Entry 2[11]

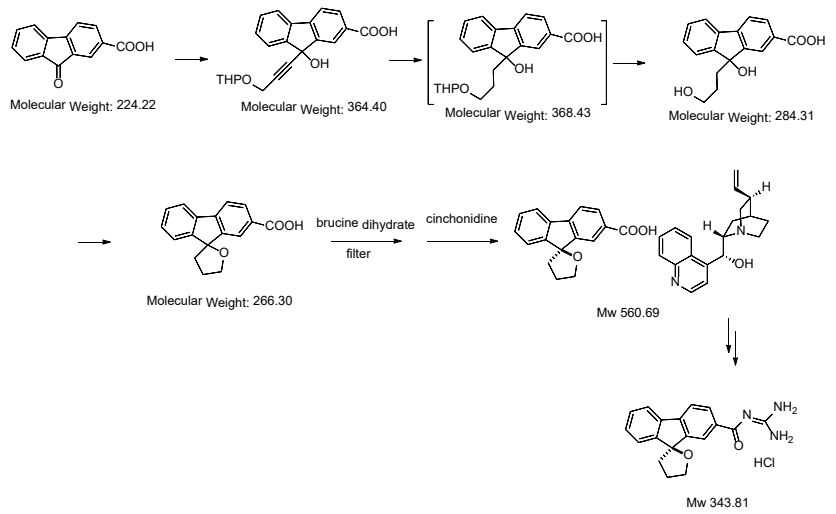
COOH
O
Molecular Weight: 224.22
THPO
OH
Molecular Weight: 364.40
Molecular Weight: 368.43
HO
Molecular Weight: 284.31
brucine dihydrate
filter
cinchonidine
Molecular Weight: 266.30
Mw 560.69
NH2
HCl
Mw 343.81

Entry 3[12]

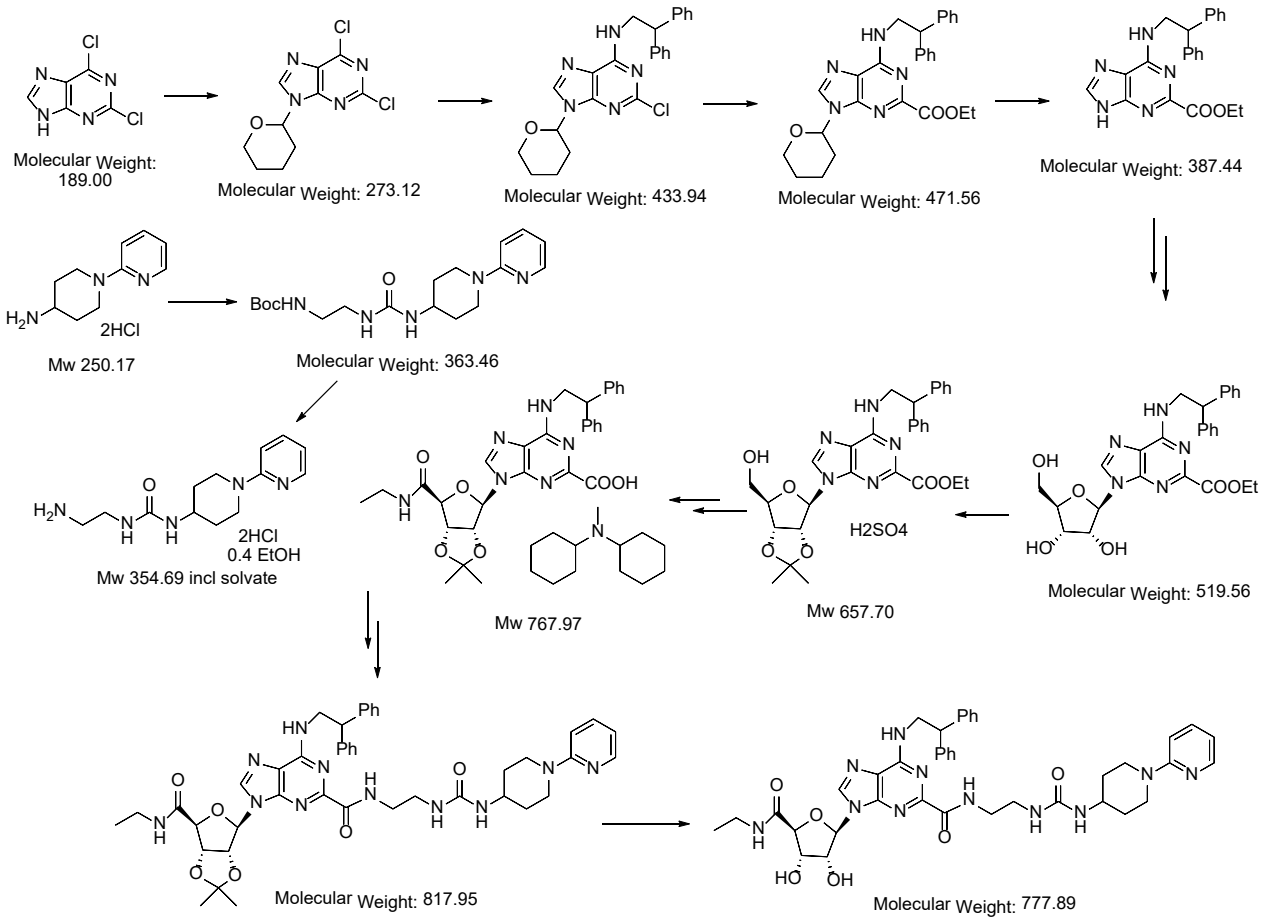
Cl
N
H
Molecular Weight: 189.00
Molecular Weight: 273.12
HN
Ph
Molecular Weight: 433.94
COOEt
Molecular Weight: 471.56
Molecular Weight: 387.44
H2N
2HCl
Mw 250.17
BocHN
Molecular Weight: 363.46
0.4 EtOH
Mw 354.69 incl solvate
COOH
Mw 767.97
OH
H2SO4
Mw 657.70
HO
Molecular Weight: 519.56
Molecular Weight: 817.95
Molecular Weight: 777.89

Entry 4.[13]

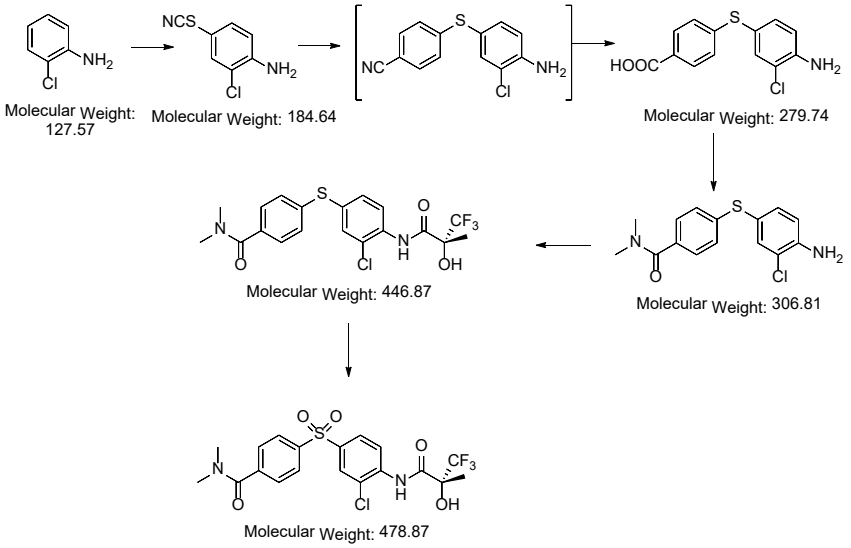

Entry 5.[14]

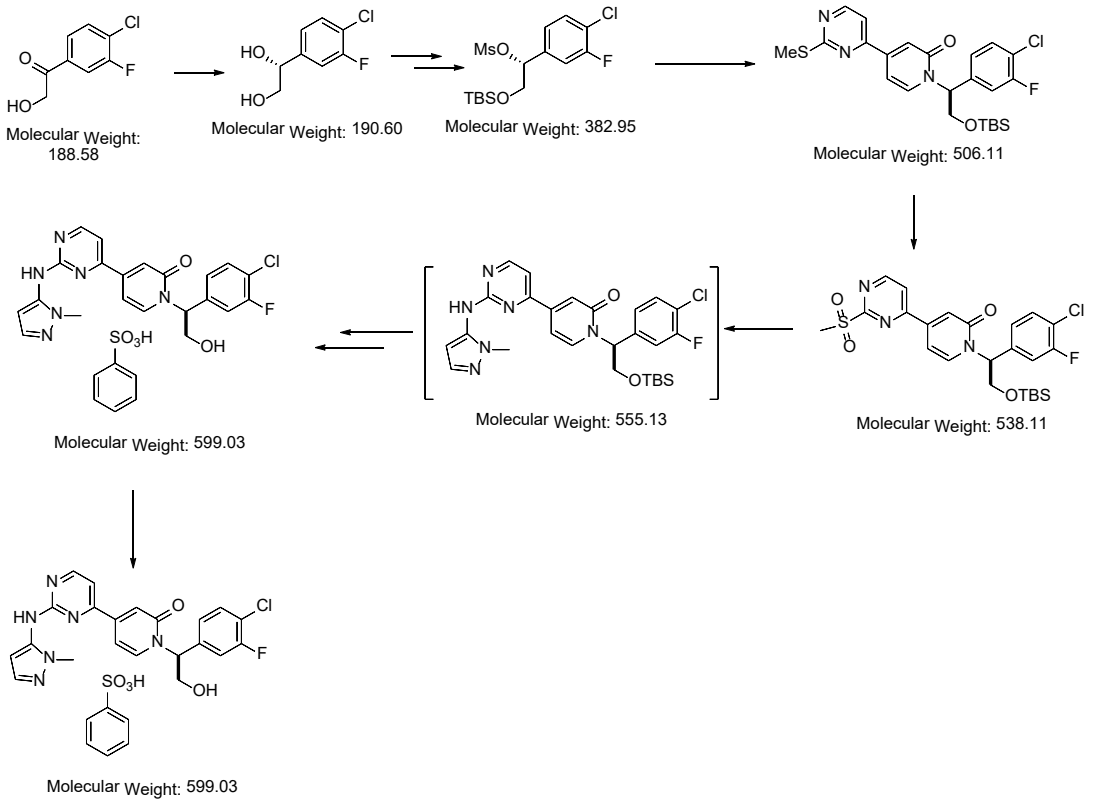
Molecular Weight: 188.58
Molecular Weight: 190.60
Molecular Weight: 382.95
Molecular Weight: 506.11
Molecular Weight: 538.11
Molecular Weight: 555.13
Molecular Weight: 599.03
Molecular Weight: 599.03

Entry 6.[15]

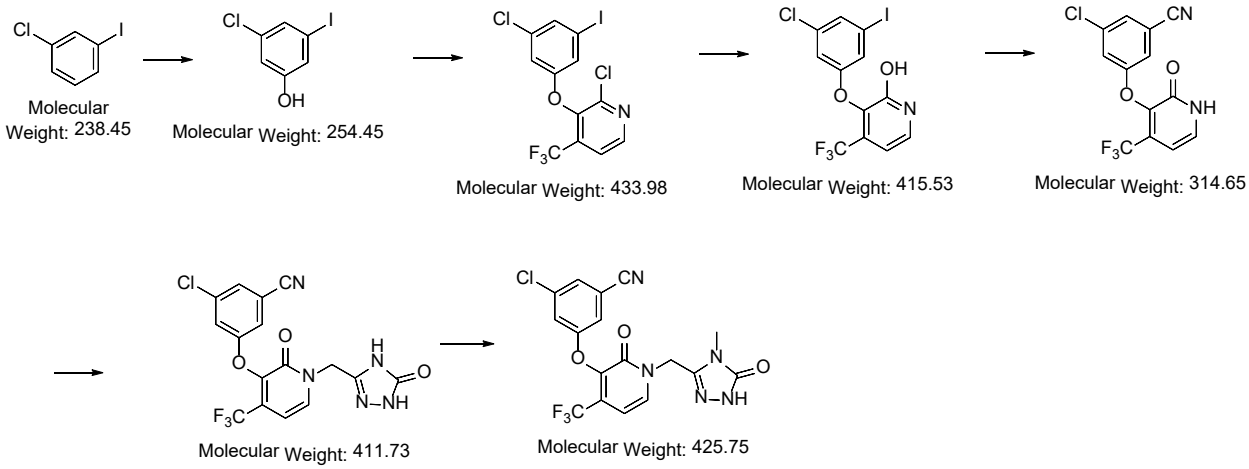
Molecular Weight: 238.45
Molecular Weight: 254.45
Molecular Weight: 433.98
Molecular Weight: 415.53
Molecular Weight: 314.65
Molecular Weight: 411.73
Molecular Weight: 425.75

Entry 7[16]

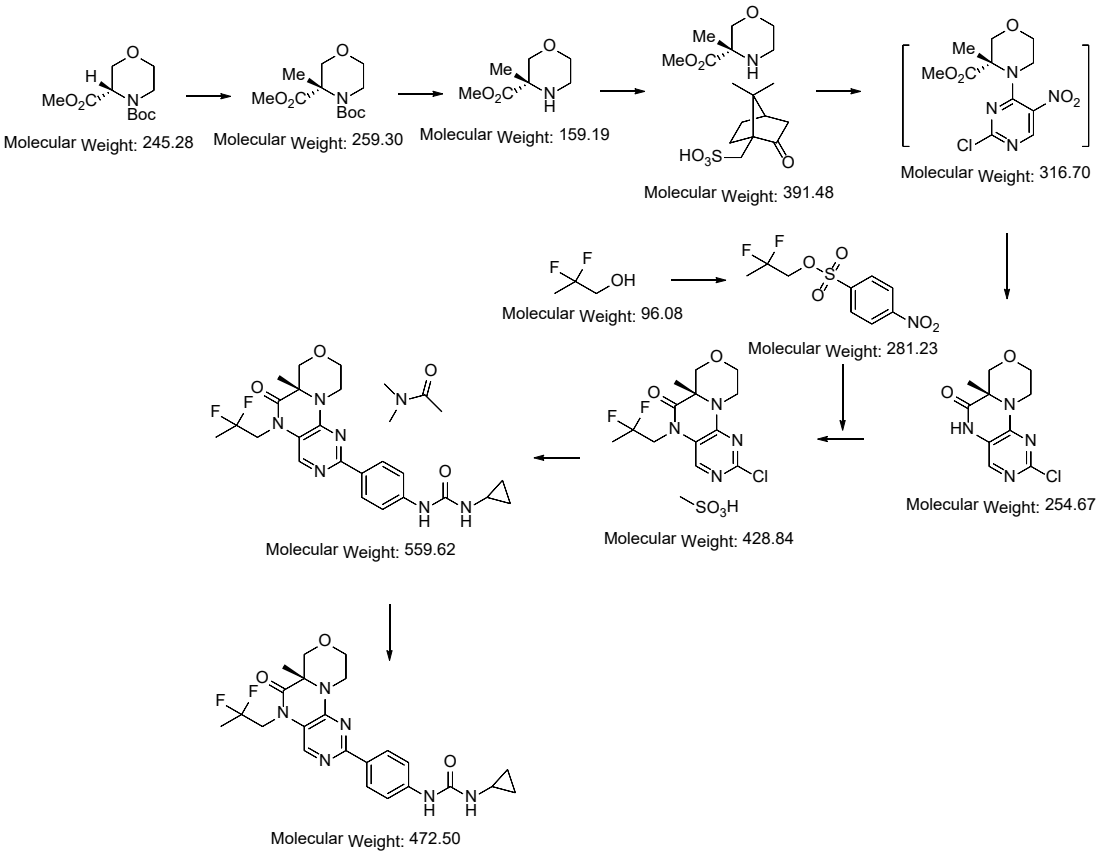

Entry 8[17]

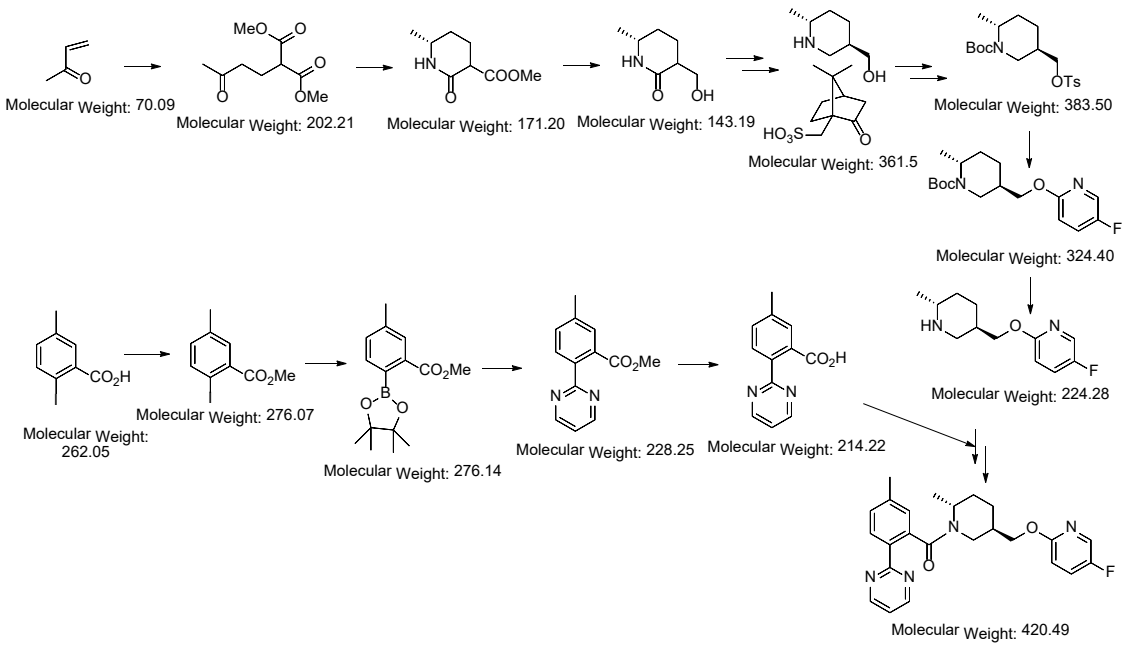

Entry 9[18]

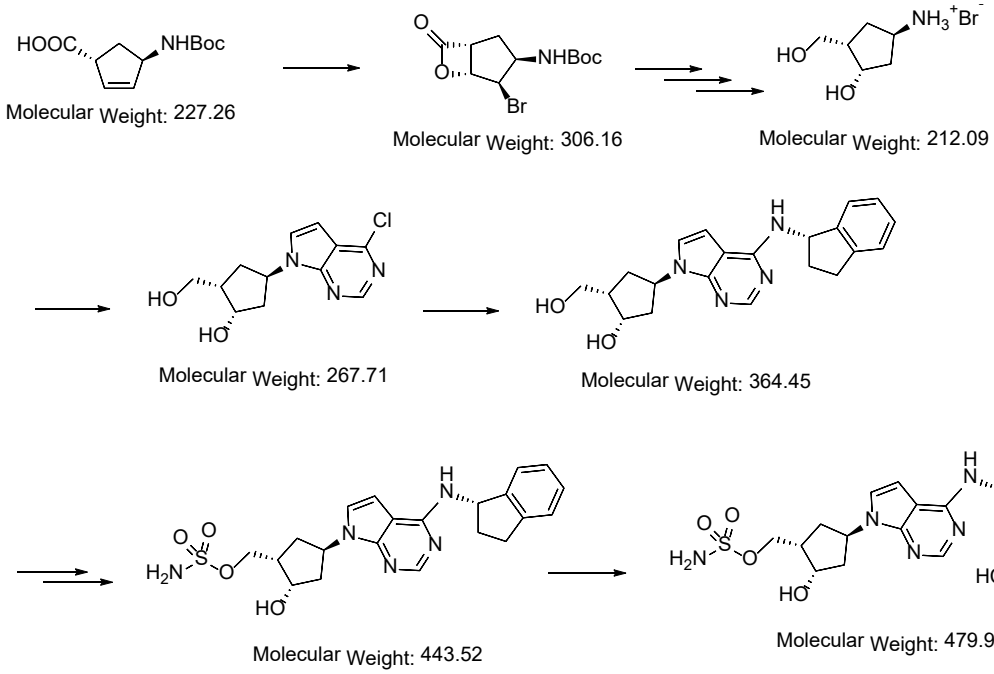

Entry 10[19]

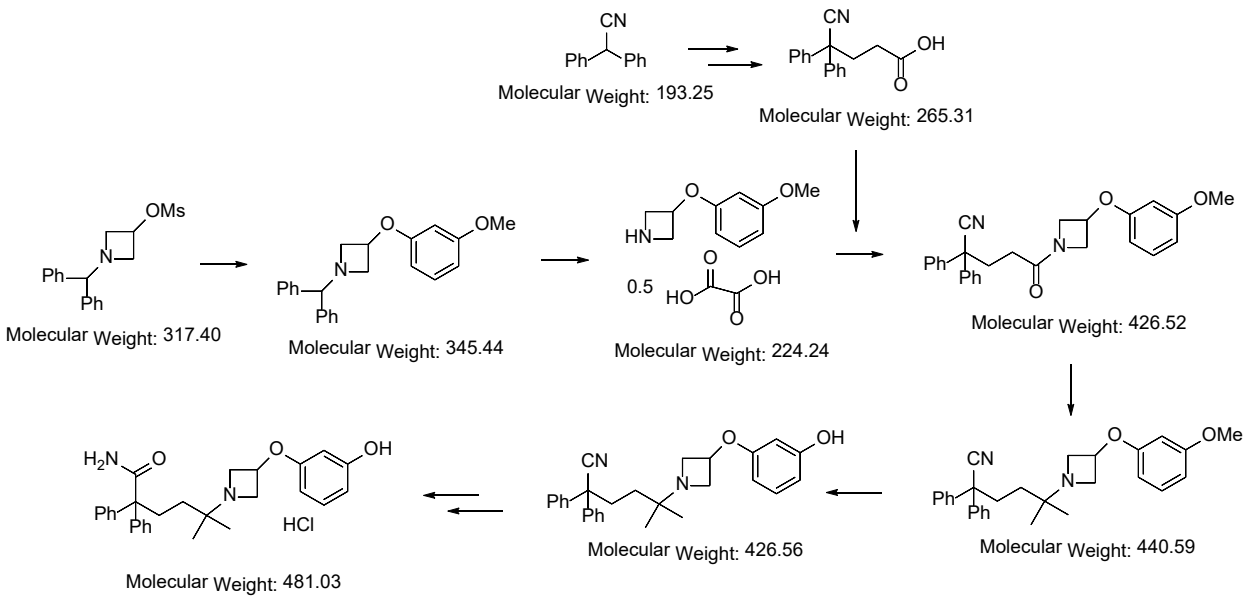

Entry 11[20]

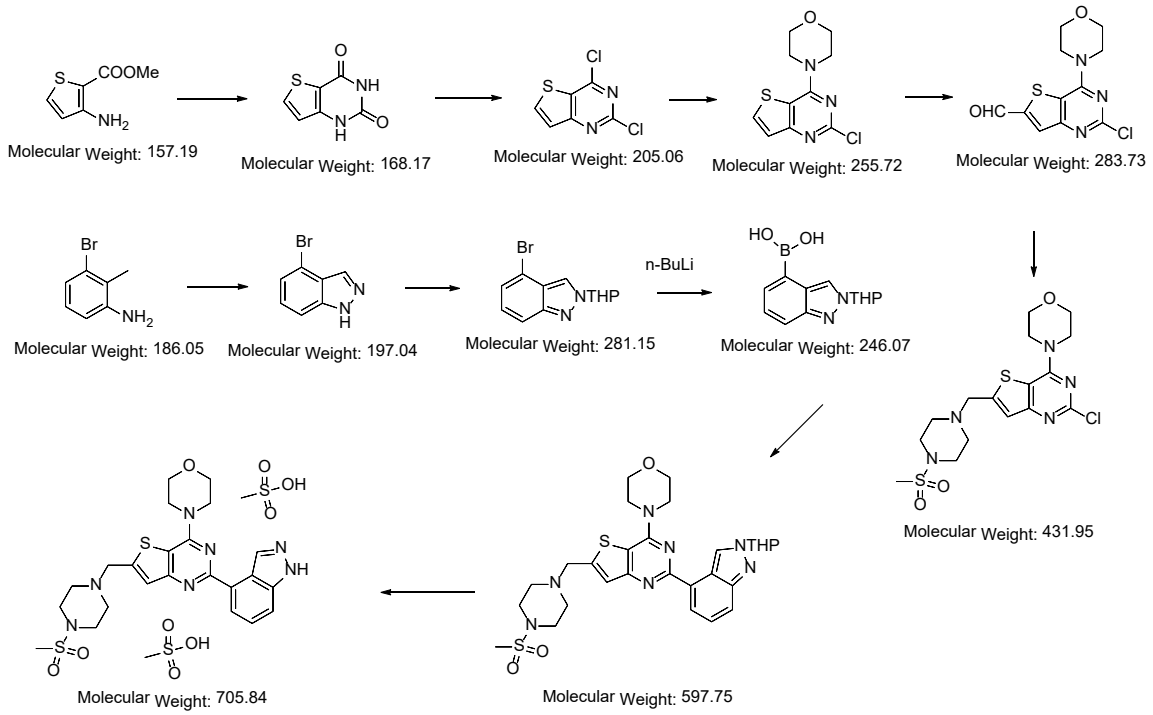

Entry 12[21]

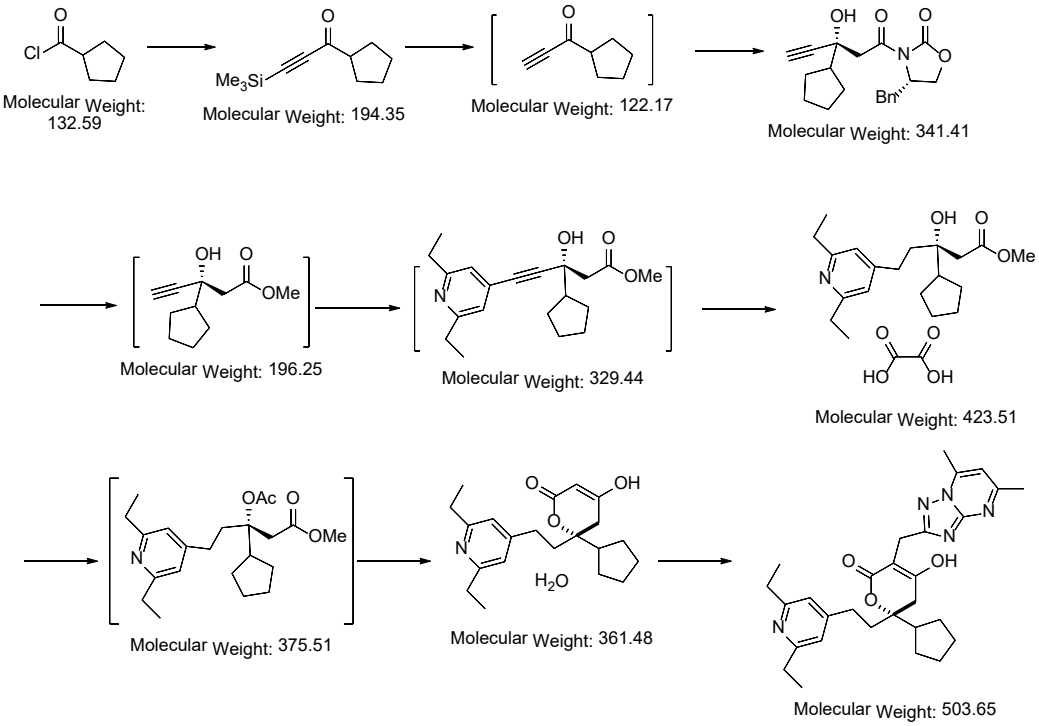
Molecular Weight: 132.59
Molecular Weight: 194.35
Molecular Weight: 122.17
Molecular Weight: 341.41
Molecular Weight: 196.25
Molecular Weight: 329.44
Molecular Weight: 423.51
Molecular Weight: 375.51
Molecular Weight: 361.48
Molecular Weight: 503.65

Entry 13[22]

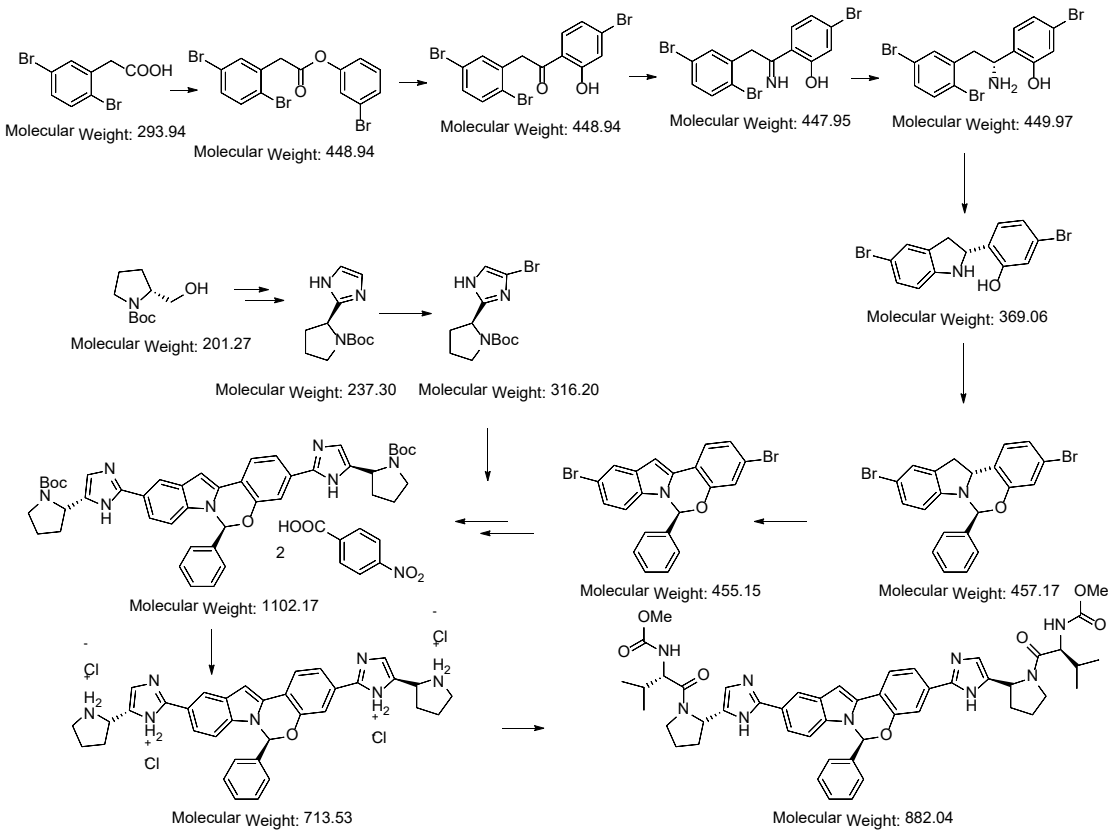
Molecular Weight: 293.94
Molecular Weight: 448.94
Molecular Weight: 448.94
Molecular Weight: 447.95
Molecular Weight: 449.97
Molecular Weight: 369.06
Molecular Weight: 201.27
Molecular Weight: 237.30
Molecular Weight: 316.20
Molecular Weight: 455.15
Molecular Weight: 457.17
Molecular Weight: 1102.17
Molecular Weight: 713.53
Molecular Weight: 882.04

Entry 14[23]

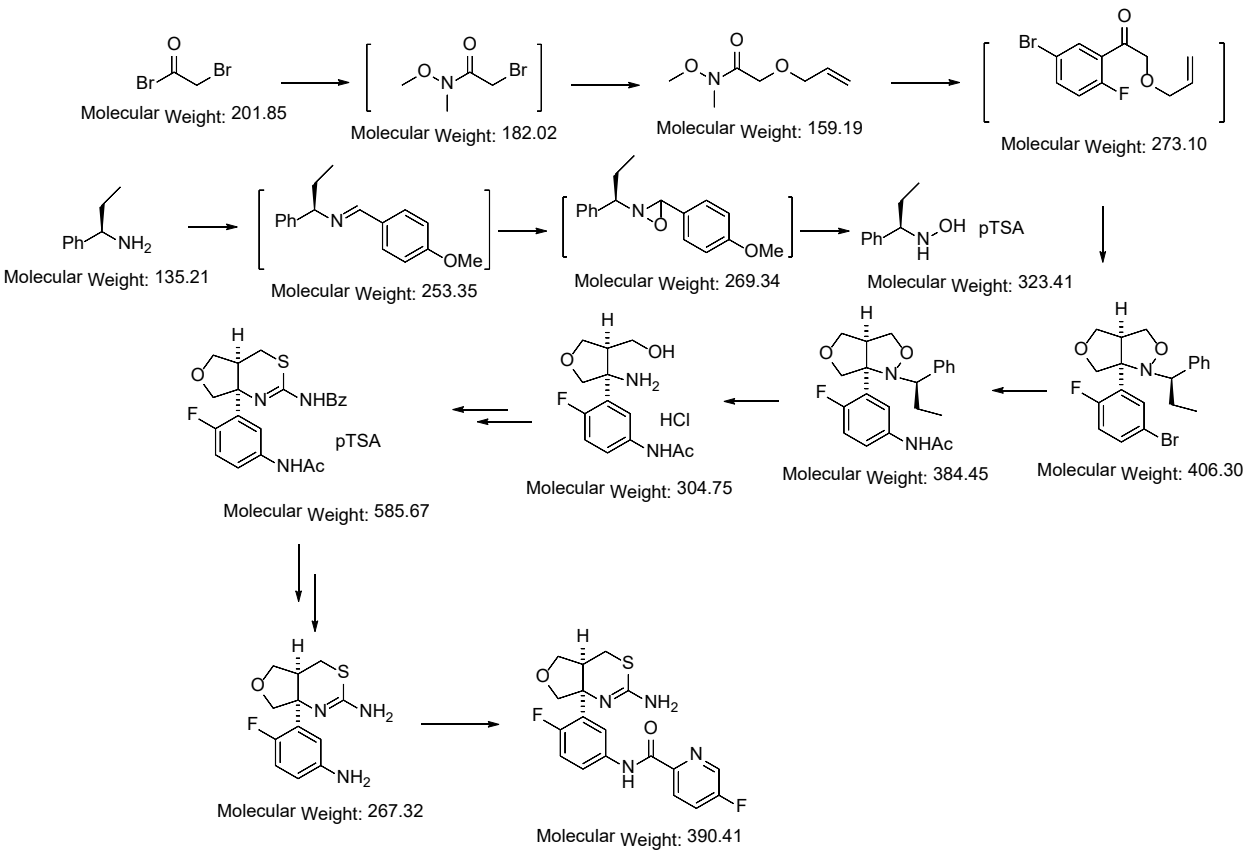

Entry 15[24]

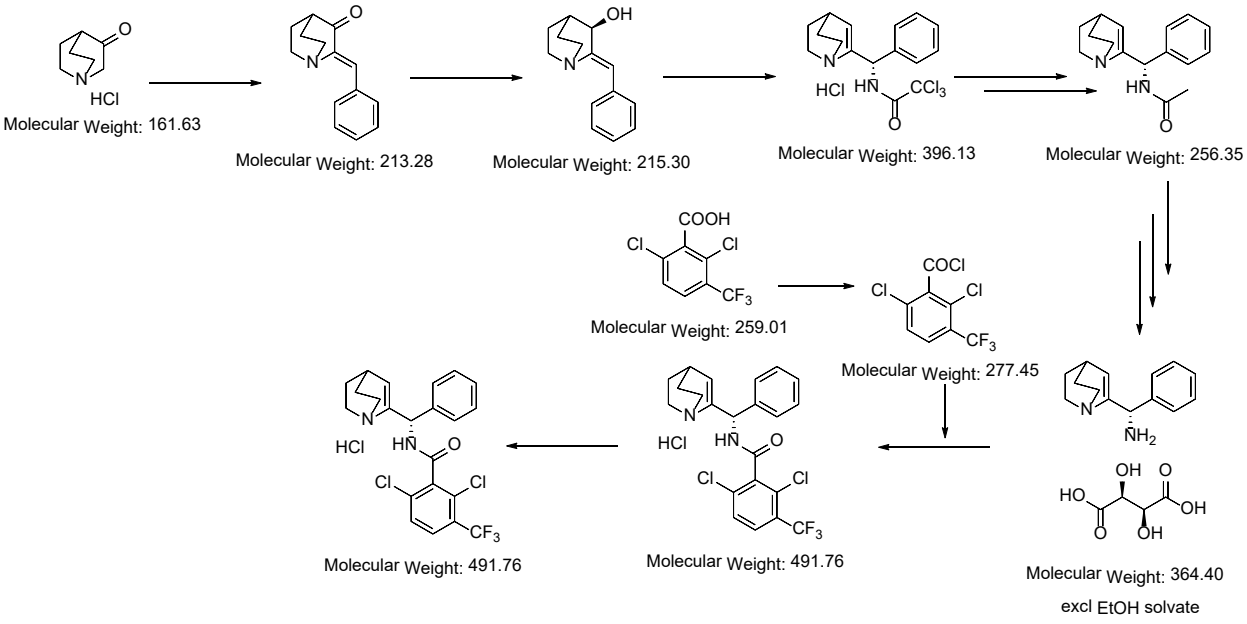

[1] (a) Chang, Cheng, J., Allaire, J., Xie, Y., McPherson, J. (2017). Shiny: Web Application Framework for R. R package version 1.0.5. https://CRAN.R-project.org/package=shiny (b) Knut Sveidqvist, Mike Bostock, Chris Pettitt, Mike Daines and Richard Iannone (2017). DiagrammeR: Graph/Network Visualization. R package version 0.9.2. https://CRAN.R-project.org/package=DiagrammeR (c) Hadley Wickham (2007). Reshaping Data with the reshape Package. Journal of Statistical Software, 21(12), 1-20. UR http://www.jstatsoft.org/v21/i12/. (d) H. Wickham. ggplot2: Elegant Graphics for Data Analysis. Springer-Verlag New York, 2009. (e) Hadley Wickham and Jennifer Bryan (2018). readxl: Read Excel Files. R package version 1.1.0. https://CRAN.R-project.org/package=readxl

[2] N. Hoshiyaa, S. L. Buchwald, *Adv. Synth. Catal*. 2012, **354**, 2031 – 2037.

[3] Roschangar, F., Sheldon, R. A., Senanayake, C. H. Overcoming barriers to green chemistry in the pharmaceutical industry – the Green Aspiration Level™ concept. *Green Chem.* **17**, 752-768 (2015).

[4] (a) A. E. Feiring et al *J. Org. Chem*. 1975, **40**, 2543. (b) R. A. Glennon et al *J. Med. Chem.* 1982, **25**, 1163.

[5] (a) Winston Chang, Joe Cheng, JJ Allaire, Yihui Xie and Jonathan McPherson (2017). shiny: Web Application Framework for R. R package version 1.0.5. https://CRAN.R-project.org/package=shiny

[6] (a) Brown, D. G.; Bostrom, J. *J. Med. Chem*. **2016**, *59*, 4443−4458; (b) Roughley, S. D.; Jordan, A. M. *J. Med. Chem*. **2011**, *54* , 3451−3479. (c) Schneider, N.; Lowe, D.; Sayle, R. A.; Landrum, G. A.,*J. Chem. Inf. Model*. **2015**, *55*, 39−53

[7] Magno, J.; Dunetz, J. R. Chem. Review. **2011**, *111*, 2177-2250.

[8] Yu, M; Lou, S.; Gonzalez-Bobes F. *Org Process Res. Dev.* **2018** *22*, 918-946.

[9] Xu, F.; Zhong, Y.-L.; Li, H.; Qi, J.; Desmond, R.; Song, Z. J.; Park, J.; Wang, T.; Truppo, M.; Humphrey, G. R.; Ruck, R. T. *Org. Lett*. **2017** *19*, 5880-5883.

[10] (*a*) Lobben, P. C., Barlow, E., Bergum, J. S., Braem, A., Chang, S.-Y., Gibson, F., Kopp, N., Lai, C., LaPorte, T. L., Leahy, D. K., Müslehiddinoğlu, J., Quiroz, F., Skliar, D., Spangler, L., Srivastava, S., Wasser, D., Wasylyk, J., Wethman, R., Xu, Z. Control Strategy for the Manufacture of Brivanib Alaninate, a Novel Pyrrolotriazine VEGFR/FGFR Inhibitor. *Org. Process. Res. Dev*. **19**, 900-907 (2015). (*b*) Pesti, J. A., LaPorte, T., Thornton, J. E., Spangler, L. , Buono, F., Crispino, G., Gibson, F., Lobben, P. C., Papaioannou, C. G. Commercial Synthesis of a Pyrrolotriazine–Fluoroindole Intermediate to Brivanib Alaninate: Process Development Directed toward Impurity Control. *Org. Process. Res. Dev*. **18**, 89-102 (2014). (*c*) LaPorte, T. L., Spangler, L., Hamedi, M., Lobben, P. C., Chan, S. H., Muslehiddinoglu, J., Wang, S. S. Y. Development of a Continuous Plug Flow Process for Preparation of a Key Intermediate for Brivanib Alaninate. *Org. Process. Res. Dev*. **18**, 1492-1502 (2014).

[11] Yoshida, S., Kasai, M., Kimura, T., Akiba, T., Takahashi, T., Sakamoto, S. Development of a Practical and Scalable Synthesis of a Potent Selective Dual Antagonist for 5-HT2B and 5-HT7 Receptors. *Org. Process Res. Dev*. **16**, 654−663 (2012).

[12] Ashcroft, C. P., Dessi, Y., Entwistle, D. A., Hesmondhalgh, L. C., Longstaff, A., Smith, J. D. Route Selection and Process Development of a Multikilogram Route to the Inhaled A2a Agonist UK-432,097. *Org. Process Res. Dev*. **16**, 470−483 (2012).

[13] Patel, B., Firkin, C. R., Snape, E. W., Jenkin, S. L., Brown, D., Chaffey, J.G.K, Hopes,P.A., Reens, C. D., Butters, M., Moseley, J. D. Process Development and Scale-Up of AZD7545, a PDK Inhibitor. *Org. Process Res. Dev*. **16**, 447−460 (2012)

[14] Xin, L., Wong, N., Iding, H., Jost, V., Zhang, H., Koenig, S. G., Sowell, C. G., Gosselin F. Development of a Practical Synthesis of ERK Inhibitor GDC-0994. *Org. Process Res. Dev*. **21**, 387−398 (2017).

[15] Campeau, L.-C., Chen, Q., Gauvreau, D., Girardin, M., Belyk, K., Maligres, P., Zhou, G., Gu, C., Zhang, W., Tan, L., O'Shea, P. D., A Robust Kilo-Scale Synthesis of Doravirine. *Org. Process Res. Dev*. 20, 1476−1481 (2016).

[16] Hicks,F., Hou, Y., Langston, M., McCarron, A., O'Brien, E., Ito, T., Ma, C., Matthews, C.,O'Bryan, C., Provencal, D., Zhao, Y., Huang, J., Yang, Q, Li, H., Johnson, M., Yan, S., Liu, Y. Development of a Practical Synthesis of a TORC1/2 Inhibitor: A Scalable Application of Memory of Chirality. *Org. Process Res. Dev*. **17**, 829−837 (2013).

[17] Girardin, M., Ouellet, S. G., Gauvreau, D., Moore, J. C., Hughes, G. Devine, P. N., O'Shea, P. D., Campeau, L.-C. Convergent Kilogram-Scale Synthesis of Dual Orexin Receptor Antagonist. *Org. Process Res. Dev*. **17**, 61−68 (2013).

[18] Dillon, B. R., Roberts, D. F., Entwistle, D. A., Glossop, P. A., Knight, C. J., Laity, D. A., James, K., Praquin, C. F., Strang, R. S., Watson, C. A. L. Development of a Scaleable Synthesis of a Geminal Dimethyl Tertiary Amine as an Inhaled Muscarinic Antagonist for the Treatment of COPD. *Org. Process Res. Dev*. **16**, 195−203 (2012).

[19] Tian, Q., Cheng, Z., Yajima, H. M., Savage, S. J., Green, K. L., Humphries, T., Reynolds, M. E., Babu, S., Gosselin, F., Askin, D., Kurimoto, I., Hirata, N., Iwasaki, M., Shimasaki, Y., Miki, T. A Practical Synthesis of a PI3K Inhibitor under Noncryogenic Conditions via Functionalization of a Lithium Triarylmagnesiate Intermediate. *Org. Process Res. Dev*. **17**, 97−107 (2013).

[20] Armitage, I., Elliott, E., L., Hicks, F., Langston, M., McCarron, A., McCubbin, Q. J., O'Brien, E., Stirling, M., Zhu, L., Process Development and GMP Production of a Potent NAE Inhibitor Pevonedistat. *Org. Process Res. Dev*. **19**, 1299−1307 (2015).

[21] Singer, R. A., Ragan, J. A., Bowles, P., Chisowa, E., Conway, B. G., Cordi, E. M., Leeman, K. R., Letendre, L. J., Sieser, J. E., Sluggett, G. W., Stanchina, C. L., Strohmeyer, H., Blunt, J., Taylor, S., Byrne, C., Lynch, D., Mullane, S., O'Sullivan, M. M., Whelan, M. Synthesis of Filibuvir. Part I. Diastereoselective Preparation of a β-Hydroxy Alkynyl Oxazolidinone and Conversion to a 6,6-Disubstituted 2H-Pyranone. *Org. Process Res. Dev*. **18**, 26−35 (2014).

[22] Mangion, I, K., Chen, C.-Y., Li, H., Maligres, P., Chen, Y., Christensen, M., Cohen, R., Jeon, I., Klapars, A., Krska, S., Nguyen, H., Reamer, R. A., Sherry, B. D., Zavialov, I. Enantioselective Synthesis of an HCV NS5a Antagonist. *Org. Lett.* **16**, 2310-2313 (2014).

[23] Kolis, S. P., Hansen, M. M., Arslantas, E., Brändli, L., Buser, J., DeBaillie, A. C., Frederick, A. L., Hoard, D. W., Hollister, A., Huber, D., Kull, T., Linder, R. J., Martin, T. J., Richey, R. N., Stutz, A., Waibel, M., Ward, A. J., Zamfir, A. Synthesis of BACE Inhibitor LY2886721. Part I. An Asymmetric Nitrone Cycloaddition Strategy. *Org. Process Res. Dev*. **19**, 1203−1213 (2015).

[24] Chandramouli, S. V., Ayers, T. A., Wu, X.-D., Tran, L. T., Peers, J. H., Disanto, R., Roberts, F., Kumar, N., Jiang, Y., Choy, N., Pemberton, C., Powers, M. R., Gardetto, A. J., D'Netto, G. A., Chen, X., Gamboa, J., Ngo, D., Copeland, W., Rudisill, D. E., Bridge, A. W., Vanasse, B. J., Lythgoe, D. J. Scale-Up of an Enantioselective Overman Rearrangement for an Asymmetric Synthesis of a Glycine Transporter 1 Inhibitor. *Org. Process Res. Dev*. **16**, 484−494 (2012).